Chapter 3

Problems of Fourier Transform Mass Spectrometry

A Route to Instrument Improvements

Richard P. Grese, Don L. Rempel, and Michael L. Gross[1]

Midwest Center for Mass Spectrometry, Department of Chemistry, University of Nebraska, Lincoln, NE 68588

Progress in FTMS is tied to understanding dynamics in ion traps. A three stage approach is envisioned: (1) modeling of ion dynamics, (2) developing tests of models by measuring ion motion in various cells, and (3) implementing new instrumentation such as improved cells and methods of excitation. Elements of this cycle are addressed with respect to five different problems. The first, nonuniform tuning over wide mass ranges, is attributed in part to z-mode excitation. A second problem is temporal variation of an inert ion signal which may lead to inaccurate kinetic results in ion-molecule reaction studies. Systematic errors in mass measurement represent the third problem. Low mass resolution for high mass ions and for ion selection in MS/MS experiments are the fourth and fifth problems that are addressed.

Although there are many attractive features of Fourier transform mass spectrometry (FTMS), there are problems with current implementations. The FT mass spectrometer is still a relatively young instrument when compared to the double-focussing mass spectrometer, and comparisons of the spectrometers and their development histories are informative and encouraging. As the attention paid to problems of earlier single-focussing instruments led to the double-focussing mass spectrometer, for example, investigation of FTMS problems now will lead to better implementations of FTMS. Here, we describe some examples, not all of them complete, of systematic attempts to investigate problems in current implementations of FTMS with an eye on improvement of the instrument.

Comparison with Sector Instruments. Modern double-focussing mass spectrometers have a long history of development, which was recently reviewed (1). The instrument has evolved through a long series of complex and interweaving events beginning with the early experiments of J. J. Thomson (2) and the first mass spectrographs of

---

[1] Correspondence should be addressed to this author.

0097-6156/87/0359-0034$07.25/0

Dempster in 1918 (3) and Aston in 1919 (4). Early instruments were used to measure atomic masses, and much effort was devoted to increase the resolution of the measurements. To improve resolution, techniques for reduction of the effects of velocity and angular dispersion at neighborhoods of focal points or planes were introduced. For example, the double-focussing instrument first developed by Bartky and Dempster in 1929 was designed to solve problems caused by the energy spread of the ion beam (5). This might be viewed as the introduction of symmetry: ideally we would want an analytical instrument to be invariant to (symmetrical with respect to) all variables except the one being measured. Another example of the use of symmetry in mass spectrometry is the improvement of resolution in time-of-flight instruments by addition of the reflectron. Sector mass spectrometer development still continues; for example, extending the upper range mass limit is an exciting development (6). Techniques employed in recent designs include inhomogeneous magnets, quadrupole lenses, non-normal poleface boundaries, non-ferrous electromagnets (7), and new and more efficient ion sources.

Over sixty years have passed since the beginning of the development of the mass spectrometer as a modern analytical instrument. In comparison, FTMS is a relatively new technique, first introduced by Comisarow and Marshall in 1974 (8). Perhaps it is an indication of the technique's high potential that FTMS has developed so rapidly. However, it should not be surprising, by analogy with the long development of sector instruments, that its full potential has not yet been realized.

Double-focussing instruments have set the standard by which other mass spectrometers, including FT mass spectrometers, are judged. High resolution, parts-per-million mass accuracy, picogram detection limits, and high mass limits (ca. 10,000 u) are attributes shared by both sector and FT mass spectrometers (9). However, achieving high performance is reasonably routine with sector instruments but not yet with FT mass spectrometers.

Resolutions of 500,000 have been reported by Ogata and Matsuda for a sector mass spectrometer (10). Resolving powers of 10^5 are trivial to obtain even with low field electromagnet-based FT systems and resolutions as high as 10^8 for an ion of m/z 18 were reported in a high field FTMS (11). Although the resolution for FTMS is higher, there may be an analogy between mass resolution achievements with sector and FT mass spectrometers. For the sector instrument, the resolution was achieved, in part, by making the spectrometer larger. In a sense, this is the same as reducing electric field problems by turning to higher magnetic fields in FTMS, an approach that does not involve the introduction of symmetry.

Because of the respect accorded high resolution sector instruments, the early reports of high resolution with FTMS raised high expectations. It was expected that the higher mass resolution would lead to high mass accuracy. Yet there are *no* reports of analytical applications in which mass measurement accuracies in FTMS (12) are significantly better than the ppm accuracies achieved for sector machines. Thus, the higher resolution capabilities of FTMS have yet to be translated into mass measurements more accurate than those available from sector machines. Because FTMS is no better, the current accomplishments in mass measurement accuracy are not noteworthy.

The sensitivity of FTMS is also comparable to that of sector instruments. Although sector instrument detectors can be used to count single ions and FTMS detectors cannot, both methods will yield a peak profile for approximately 100 ions. Detecting a single ion in organic or bioanalytical chemistry is of limited utility because its mass cannot be assigned with any certainty.

In addition to the characteristics shared by FTMS and sector MS, FT mass spectrometers have several advantages over sector instruments. These advantages have been cited often and they include (9b): 1) ion trapping and manipulation, 2) multichannel advantage, 3) high resolution with no loss in sensitivity, 4) compatibility with pulsed devices (e.g. lasers, pulse valves), and 5) multiple MS/MS experiments (MS^n). Some of these advantages are shared by time-of-flight instruments; however, TOF does not give high resolution or permit accurate mass determinations. Another advantage of FTMS is the approximate mass invariance of the signal intensity (13-14) for a given number of ions and circumstances. This contrasts with the mass discrimination (15) which occurs for multipliers that are used in sector machines.

Status of FTMS. Since its introduction in 1974, FTMS has been demonstrated to be capable of solving a wide variety of chemical problems that are not possible to solve by using other mass spectrometers. For example, analytical applications have been designed to take advantage of the multichannel advantage and the ultra high resolution capabilities of FTMS (16). Ultra high resolution was demonstrated with chemical ionization (17-18), GC/MS (19), multi-photon ionization (MPI) (20), MPI-GC/MS (20), and laser desorption (21). A recent application of FTMS is GC/MS of olefins that are chemically ionized with Fe^+ ions which are produced by pulsed laser multiphoton dissociation/ionization of $Fe(CO)_5$ (22). However, much of the research has not addressed fundamental problems in the understanding of the behavior of ions in a cubic cell. Because of our incomplete knowledge of ion dynamics, FTMS remains nonroutine with respect to a number of items. 1) The upper end of the dynamic range is bound by the number of ions the cell can hold. A dynamic range of 10^2-10^3 has been estimated for the cubic cell; this is in contrast to conventional mass spectrometers with electron multipliers which have dynamic ranges of at least 10^5. 2) Nonuniform tuning over wide mass ranges contributes to unreliable peak heights in the mass spectrum. Correct peak heights are needed for interpretation and for optimum utilization of mass spectra library searches. 3) MS/MS experiments have been limited by poor resolution in MS-I and by poor reproducibility of activation methods. 4) Soft ionization methods have not been routine with FTMS. The use of external sources may be the expedient but not long range solution to this problem.

Route to Improvement. As one route to solving problems that perplex FTMS, we have made use of a systematic approach illustrated in Figure 1. The "Development Cycle" enables us to define clearly problems and to arrive at solutions through an organized combination of theoretical and experimental work. The most difficult aspect of

---

this approacl
start with
problems and
cyclic natur
provide a
performance,
accurate mode
In the
approach has

Solving Probl

Nonuniform Tu
motivation fc
when problems
Two such prob
mass ranges (
occurring at
necessary for
z-mode excita
Some me
particular,
z-excitation
excitation of
eliminating
trapping mode
are significa
mode.
However,
with frequenc
is essential
exaggerated i
cyclotron orb
excitation pl
trapping plat
their cyclotr
bottom plate r
plate. This
of the excitat
an average fo
the z-mode osc
ion is lost fr
2. Model:
the average fc

F

F = avera
E_z = elec
V_p = ampl
z = ion p
a = lengt
A_r = radi
ϕ = phase

this approach is knowing how to start. An obvious approach is to start with defining the problem; however, multiple causes of problems and mixed symptoms have slowed progress. Once begun, the cyclic nature of this approach grows outward. Improved models provide a basis for design changes that improve instrument performance, and understanding the actual performance leads to more accurate models.

In the remaining sections, specific examples of how this approach has led to instrument improvements are given.

Solving Problems Facing FTMS

Nonuniform Tuning of Mass Spectra (23). 1. Problem Definition: The motivation for improving our understanding of FTMS develops often when problems arise that limit the accuracy of experimental results. Two such problems: 1) nonuniform tuning for peak heights over wide mass ranges (24), and 2) ion losses in double resonance experiments occurring at excitations insufficient to raise the ion to a radius necessary for ejection (25), have led us to an investigation of z-mode excitation as a possible cause.

Some mechanisms of z-mode excitation are known; and in particular, Beauchamp and Armstrong's (26) direct method of z-excitation can be used for double resonance. Fortunately, excitation of the z-mode via these processes can be avoided by eliminating the excitation frequency components to which the trapping mode respond. This is possible because these frequencies are significantly different than those used to excite the cyclotron mode.

However, excitation of the z-oscillation mode may also occur with frequency components near or at the cyclotron frequency which is essential for excitation of the cyclotron mode. As is exaggerated in Figure 2, when the ions are at the top of the cyclotron orbit, there is a peak positive potential on the top excitation plate that results in a component force toward the trapping plates. Similarly, when the ions are at the bottom of their cyclotron orbit, there is a peak positive potential on the bottom plate resulting also in a component force toward the trapping plate. This synchronization of temporal changes in the z-component of the excitation field and the spatial motion of the ion results in an average force that changes the trapping motion. The energy of the z-mode oscillation might even be modified to the point where the ion is lost from the cell.

2. Model: A simple model (Equation 1) was employed to depict the average force that modifies the z-motion during excitation.

$$F = qE_z \sim qkV_p[z/a][A_r/a](1 - [A_r/a]^2)\cos\phi \qquad (1)$$

F = average force that modifies the z-motion of the ion
E_z = electric field
V_p = amplitude of excitation waveform
z = ion position along the z-axis (z = 0 at the cell center).
a = length of inside edge of cubic cell
A_r = radius of cyclotron orbit
ϕ = phase of excitation waveform

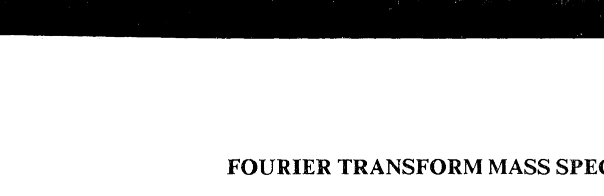

Figure 1. Development cycle for instrument improvements in FTMS.

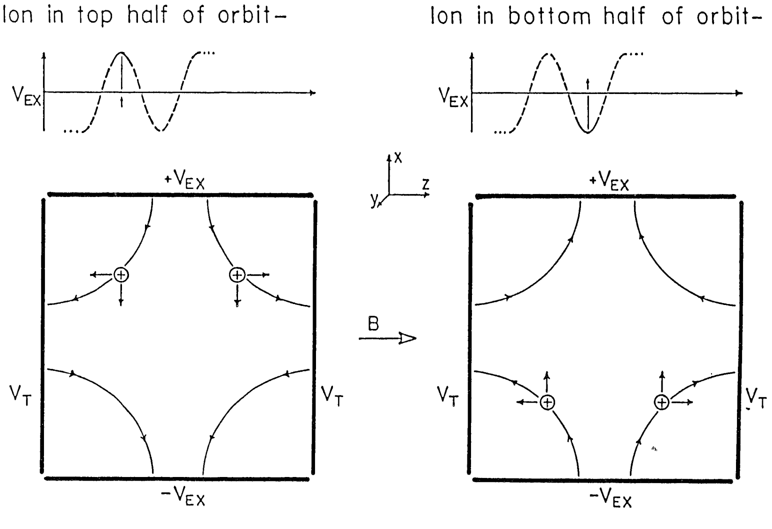

Figure 2. The synchronization between rf excitation waveform and ion cyclotron motion shown with exaggerated phase; i.e. $\phi \neq \pm \pi/2$. (Reproduced with permission from Ref. 23 Copyright 1986 Elsevier Science Publishers B.V.)

Several t
1) The perturb
amplitude V_p.
for the high a
bandwidths in
z-position of
that reduce th
such as ion-m
z-excitation w
perturbation a
motion and the
transitory per
discriminatory.
3. Tool:
design an exper
the extreme cas
The "trap-switc
loss in the z-d
the trapping vo
trap is switche
is increased. (
between the low
high (reference)
lower voltage.
the ion signal
be lower than wh
ion loss should
test excitation.
The first m
is the loss of
test chirp excit
the excitation i
as a result of t
Several add
difference in th
(0-2000 kHz) chi
or 1.04 V at
expectation. 2)
losses than do m
excitation of th
losses decrease a
as expected fr
considerably redu
62 ms to 2.015
expected, collisi
long delay has re
Another tool
of motion. McIv
tool for studying
that mass discrim
ions were calcul
conditions for wh
calculations, the
different z-mode
base-to-peak at e

Several trends are predictable with this simplified model. 1) The perturbation of the z-motion increases with the excitation amplitude V_p. This suggests that the z-oscillation would be largest for the high amplitude rf bursts that are used to achieve greater bandwidths in FTMS. 2) The perturbation becomes smaller as the z-position of the ion goes to zero. This suggests that processes that reduce the magnitude of the z-oscillations before excitation, such as ion-molecule collisions, should reduce the undesired z-excitation when the perturbing force is transitory. 3) The perturbation also depends on the relative phase between the ion motion and the excitation waveform. This dependence suggests a transitory perturbation for chirp excitations that is mass discriminatory.

3. Tool: To demonstrate z-mode excitation, it is easiest to design an experiment that measures the phenomenon as it occurs in the extreme case; that is, ejection of the ion along the z-axis. The "trap-switch" experiment (23) (Figure 3a) determines the ion loss in the z-direction as a function of time by rapidly increasing the trapping voltage at a variable time in the sequence. As the trap is switched to a higher voltage, the threshold for z-mode loss is increased. Changes in signal reflect differences in the ion loss between the low (test) trapping voltage (0.44 or 1.04 V) and the high (reference) voltage (4 V) over the time that the trap is at the lower voltage. If there is z-mode ion loss during excitation, then the ion signal when the trap-switch occurs after excitation should be lower than when the trap-switch occurs prior to excitation. Less ion loss should be seen if a higher trapping field is on during the test excitation.

The first result of the trap-switch experiment (see Figure 3b) is the loss of signal occurring when the trap-switch is after the test chirp excitations. The decrease in signal around the time of the excitation indicates that ion loss occurred in the z-direction as a result of the excitation.

Several additional observations are made: 1) There is little difference in the number of ions lost as a consequence of wide band (0-2000 kHz) chirp excitation for trapping voltages of either 0.44 or 1.04 V at high level excitation in some variance with expectation. 2) Wide band chirps (0-2000 kHz) produce larger ion losses than do narrow band chirps (200-350 kHz), perhaps, because excitation of the magnetron mode occurs in the first case. 3) Ion losses decrease as the amplitude of the wide band chirp is decreased as expected from the simple model. 4) Ion z-ejection is considerably reduced if the test chirp excitation was delayed from 62 ms to 2.015 sec (plotted as open squares in Figure 3b). As expected, collisional damping of the z-mode amplitudes during the long delay has reduced the magnitude of z-mode excitation.

Another tool is the numerical integration of the ion equations of motion. McIver (27) and Marshall (28) have made use of this tool for studying some aspects of ion motion. Here, to corroborate that mass discriminating z-losses do occur, the trajectory of single ions were calculated under conditions chosen to imitate normal conditions for which symptoms of z-excitation are observed. For the calculations, the ions were started on the z-axis and were given different z-mode energies. The chirp excitation was 9.67 volts base-to-peak at each excitation plate with a 2.105 kHz/μsec sweep

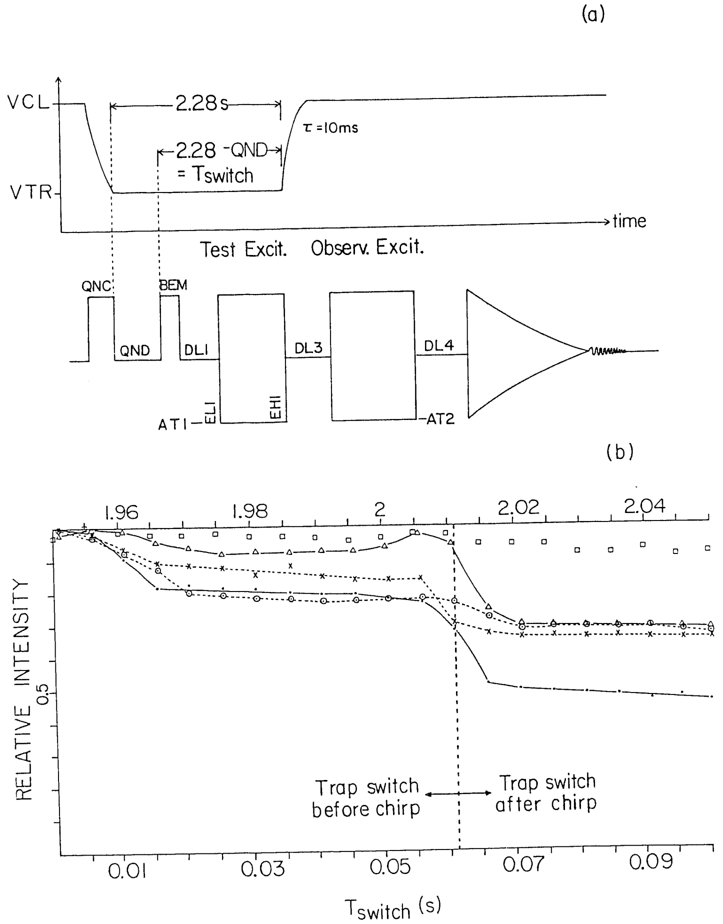

Figure 3. (a). Trap switch time sequence. (b). Relative intensity of benzene molecular ion versus trap switch time for a chirp test excitation. 100,000 ions were formed initially.

	EL1(kHz)	EH1(MHz)	AT1(dB)	VTR(V)	DL1(ms)
•---•	0	2	2	0.44	47
△---△	0	2	2	1.04	47
○---○	0	2	5	0.44	47
x...x	200	0.350	2	0.44	47
□...□	0	2	2	0.44	2000

(Reproduced with permission from Ref. 23. Copyright 1986 Elsevier Science Publishers B.V.)

---

rate and 0
magnetic fi
When t
excitation
conclusion
tried for
energy is
initial ion
lost in th
percent or
z-mode ene
initial z-m
z-mode ener
that for lo
ejected.
The nu
experiment
(CH_4^{+}) and
control exp
consecutive
essentially
detectable.
2.094 kHz/µs
$CH_4^{+}/C_6H_6^{+}$
was increase
4. Poss
performance
necessary.
suggest seve
i) Low
ions when q
essential.
ii) Exc
impart the
significant
iii) Th
before excit
involve usi
excitation o
excitation t
iv) Mod
a) Elongatin
z-component
exposed to
b) Modificat
the cubic ce
Two such mo
traps (31).
constitute
z-mode exci
fields. For
the uniform
Similarly, f
improved by
closer toge

rate and 0 to 2 MHz sweep width. Other conditions were a 1.2 T magnetic field, a 0.0254 m cubic trap, and a 1.0 V trap potential.

When the z-mode position and velocity at the beginning of the excitation is compared with the corresponding information at the conclusion of the excitation, it is found that in all the cases tried for benzene (m/q = 78) and nitrogen (m/q = 28), the z-mode energy is increased by the excitation. Those benzene ions with initial ion z-mode energies 50 percent of the trappable maximum are lost in the z-direction whereas ions with initial z-modes of 40 percent or less are not lost. Those nitrogen ions with initial z-mode energies 17.5% or more are lost whereas an ion with an initial z-mode energy of 15% is not lost. The different initial z-mode energies required for loss is consistent with the hypothesis that for lower mass ions a larger fraction of the ion population is ejected.

The numerical results are consistent with the result of an experiment in which the ion cyclotron orbit sizes of a methane ($CH_4^{+\cdot}$) and benzene ($C_6H_6^{+\cdot}$) mixture of ions were varied. In the control experiment, the two ions were excited by low amplitude consecutive RF burst pulses of varied time. The signal ratio was essentially constant over the range of orbits for which signals were detectable. In contrast, for a chirp from 10 kHz to 2 Mhz at 2.094 kHz/µsec of varied amplitude, the abundance ratio of $CH_4^{+\cdot}/C_6H_6^{+\cdot}$ decreased from about 90% to about 10% as the orbit size was increased, indicating loss of the lighter ion.

4. Possible Solutions: Because z-mode excitations degrade the performance of FTMS, methods to minimize z-mode excitations are necessary. Theoretical (Equation 1) and experimental results suggest several possible strategies.

i) Low amplitude rf bursts should be used to select specific ions when quantitation is the goal and wideband operation is not essential.

ii) Excitation pulses might be used if they are short enough to impart the momentum to the ions before they have a chance to move a significant distance from the z-axis.

iii) The ions should be confined to smaller z-mode amplitudes before exciting the cyclotron mode. Two methods to facilitate this involve using the trap-switch to compress the ion cloud prior to excitation or inserting sufficient delay time between ionization and excitation to allow collisional relaxation of the ion cloud.

iv) Modified cell designs might be used to minimize z-loss. a) Elongating the cell in the z-direction (29) should reduce the z-component electric forces and decrease the fraction of ions exposed to the larger z-components of the excitation field. b) Modification of the cell design to remove the odd symmetries of the cubic cell that cause the synchronization should also be useful. Two such modified cells are the cylindrical (30) and hyperbolic traps (31). c) Formed excitation and detection plates may constitute another cell modification for reducing the effects of z-mode excitation by improving the uniformity of the excitation fields. Formed cell plates were used by Clow and Futrell to improve the uniformity of drift velocities in a drift cell ICR (32). Similarly, for cubic cells the excitation field uniformity would be improved by bringing all the edges of two nominally parallel plates closer together to compensate for their finite area and other electrode proximity (Figure 4). The same set of plates would be used for both excitation and detection by using carefully designed switches and in that way escape the dilemma of designing one set of plates at the expense of the other.

Temporal Variation of Ion Signal of an Inert Ion. 1. Problem Definition: Several assumptions are required if correct correlations between ion signal and chemical reactivity are to be made from ion kinetic studies using FTMS. The first assumption must be that the sensitivity of the ion trap remains constant with time so that ion signals are representative of the ion population with time. The second assumption is that losses of reactant ions are due to consumption of those ions in a chemical reaction and not by physical processes.

One would expect that the signal of an unreactive ion would be invariant with time. However, the benzene molecular ion signal decreases or increases in time for correspondingly low or high trap voltages. Decreases in ion abundance are not surprising, as ion radial diffusion will occur; but the ion abundance increases shown in Figure 5 are more unexpected.

2. Model: Ion losses from an FTMS cell can occur by mechanisms other than chemical reaction and radial diffusion. Ions that have acquired sufficient kinetic energy from fragmentation processes can overcome the potential barrier of the trapping field especially when low trapping voltages are used. Ion loss owing to fragmentation was demonstrated by Riggin, et al. (34a,b).

Ion evaporation can also account for ion losses from the cell. The term "evaporation" is used to describe processes by which ion-ion collisions distribute z-mode energy with the result that some ions acquire enough kinetic energy to escape the trapping field. Ion evaporation was studied for thermal population of ions at low pressure (3×10^{-10} torr) and long delay times (100 sec) (35). Ion evaporation can be reduced with higher trap voltages that provide higher thresholds for loss. As shown in Figure 5 for the case of the benzene molecular ion, further increases in trap voltage beyond 0.74 volts produce relatively small further increases of signal with time.

After reducing the magnitude of ion evaporation, we are still left with a signal that increases in time. In this regard, ion image currents have been shown to be dependent on the position of ions cyclotroning with small orbits in rectangular traps (36). Because ions change their positions in the cell as a function of time, the signal per ion may be expected to change. Furthermore, signals from ions formed by ionization methods that are directed along axes other than the z-axis (such as laser desorption and multiphoton ionization in the cell we are using) may be affected by the different spatial distribution of the ions.

We have developed a model to explain the time dependent change in sensitivity for ions during excitation and detection. The first step is to describe the image charge displacement amplitude, $S(A_R, A_Z)$, as a function of cyclotron and z-mode amplitudes. The displacement amplitude was derived using an approximate description of the antenna fields in a cubic cell. The second step in developing the model is to derive a relationship to describe the cyclotron orbit as a function of time for an rf burst. An energy conservation

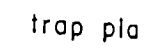

Figure 4. Exploc
excitation/detect
electrically iso

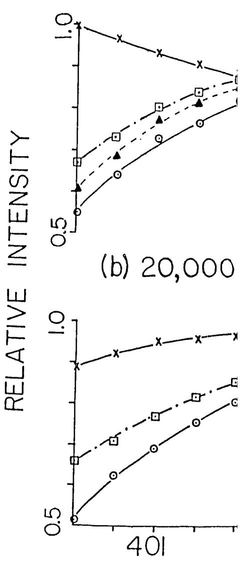

Figure 5. (a). T
of 100,000
0.44 V; ⊡, 0.7
20,000 benzene i
and ⊙, 2.04 V.
Copyright 1986 El

ates would be
'ully designed
ng one set of

n. 1. Problem
if correct
ity are to be
ssumption must
tant with time
pulation with
t ions are due
n and not by

e ion would be
ar ion signal
w or high trap
ising, as ion
ncreases shown

by mechanisms
Ions that have
processes can
eld especially
ss owing to
b).
from the cell.
sses by which
e result that
the trapping
lation of ions
100 sec) (35).
voltages that
gure 5 for the
eases in trap
ther increases

, we are still
is regard, ion
he position of
r traps (36).
a function of
Furthermore,
t are directed
desorption and
be affected by

ependent change
ion. The first
mplitude, S(A_R,
plitudes. The
ate description
p in developing
the cyclotron
gy conservation

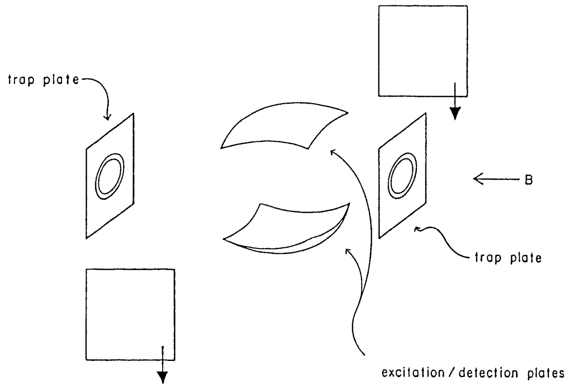

Figure 4. Exploded modified cubic trap with formed excitation/detection plates. Trap electrodes are segmented by electrically isolating a disk shaped region.

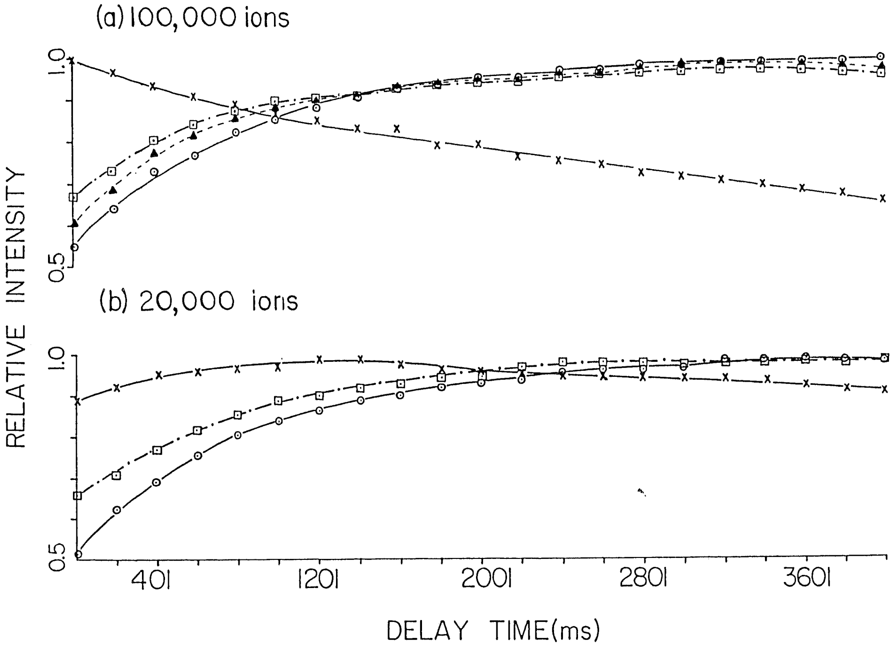

Figure 5. (a). Temporal dependence of relative signal intensity of 100,000 benzene ions at different trap voltages: x, 0.44 V; ⊡, 0.74 V; ▲, 1.04 V and ⊙, 2.04 V. (b). Initial 20,000 benzene ions at trap voltages of x, 0.44 V; ⊡, 0.74 V; and ⊙, 2.04 V. (Reproduced with permission from Ref. 33. Copyright 1986 Elsevier Science Publishers B.V.)

argument is used to deduce the cyclotron orbit sizes from the charge displacement on the excitation plates. Because the symmetry of the cubic cell requires that the charge displacement amplitude on the receiver plates be the same as on the excitation plates, the amplitude of the receiver charge displacement can also be inferred. By using the above arguments applied to a narrow band rf excitation, a relationship between A_r, the radius of the cyclotron mode, and A_z, the z-mode oscillation amplitude, can be obtained. This relationship (see Figure 6) is then used to deduce the signal, $S(A_z)$, as a function of A_z only.

The most obvious effect seen in Figure 6 is the large dependence of ion signal on ion z-oscillation amplitudes. The signal, normalized to 100% for $A_z = 0$, drops to <30% for ions grazing the trap plates. It is also apparent from Figure 6 that for ions of low A_z values, the graph is fairly flat. Thus, if the z-mode oscillation amplitude of each ion is initially confined to a low value, the signal change owing to further collisional damping of the z-mode amplitude, A_z, should be reduced. The figure also shows a weak dependence of curve shape on the size of A_r.

It is also expected that reactive collisions may diminish the effects of collisional damping of the z-oscillation. An unreactive collision removes energy from the z-mode oscillation so that the ion contributes more signal current at its original cyclotron frequency whereas a reactive collision removes an ion from a reactant population giving a true indication of the loss from the original population. The loss rate from the reactant population for ions of z-oscillation, A_z, is proportional to the density of reactant ions of amplitude A_z. Thus, for very reactive ions, no change in sensitivity due to collisional relaxation is expected.

3. Tool: According to the above model, the signal for an unreactive ion should increase as the ion cloud undergoes relaxation toward the z = 0 plane. The size of this change can be computed as a ratio of expected signals for two z-mode amplitude distributions. The first is the average of $S(A_z)$ over a z-mode amplitude distribution determined by uniform initial positions along the z axis and a thermal distribution of z velocities corresponding to the temperature of the background gas. This approximates the z-mode amplitude distribution of the benzene molecular ions generated by an electron beam assuming no collisions occur after the ion is formed. The second is the average of $S(A_z)$ over a thermal z-mode amplitude distribution determined by a quadratic potential along the z-axis and with a temperature equal to that of the background gas. Here it is assumed that ion-neutral collisions dominate to determine the second distribution.

The tool to investigate the relationship between sensitivity and z-mode relaxation is simply a measurement of the signal intensity of an unreactive species as a function of time under conditions in which evaporation and charge exchange are known to be small effects. The measured ratio of signal (just after the beam) to signal maximum (after a delay of seconds) compares reasonably well with the ratio computed by employing the assumed distributions.

4. Possible Solutions: For accurate kinetic measurements, the effect of z-mode relaxation on ion signals must be controlled. It is impractical to use long delay times between ionization and

excitation because time delay is the experimental variable. A possible solution is ion compression using a trap-switch (23). Low kinetic energy ions should be compressed to ca. the z = 0 plane by increasing the trapping potential after ionization. Figure 7 shows the effect of ion compression on the temporal behavior of the benzene molecular ion signal. The effects of z-mode relaxation at short delay times have been largely removed by the use of the trap-switch.

Systematic Errors in Accurate Mass Measurements. 1. Problem Definition: The value of high resolution mass spectrometry is diminished if the mass measurements do not give unambiguous elemental compositions. Accurate mass measurements in FTMS require a precise measurement of ion frequencies and an accurate calibration law for converting ions frequencies to mass. The ion frequencies can be measured to nine significant figures with modern electronics; however, the relationship between ion frequencies in the cubic cell and mass still requires further development.

The evolution of a calibration law for the cubic cell has seen a number of proposals for the frequency-to-mass relationship (26,37-40). Recently, Ledford, et al. (40) developed an algebraically correct mass calibration law (Equation 2), which is now commonly used. Unlike sector mass spectrometry in which many

$$m = a/f_{obs} + b/f^2_{obs} \qquad (2)$$

reference mass ions are required, only two references are required to calculate the two calibration constants, (2) a and b, which are required to relate mass, m, to the observed signal frequency, f_{obs}. This equation is sufficiently accurate to give errors in the 1-10 ppm range (12). However, in some instances, these errors are systematic and too large to give correct elemental composition assignments. Also, the systematic errors have been observed to increase with increasing number of ions. Therefore, the model does not account for all space charge effects. Nevertheless, it has been estimated that 70% of the space charge effects are accounted for (40). Space charge-related errors may limit utility of the calibration law over wide dynamic ranges of ion numbers such as are encountered in GC/FTMS.

2. Model: A quantitative model that leads to the development of an accurate calibration law is not yet readily obtainable because of the apparent complexity in the frequency variations in the cubic cell. Frequency variations have been studied by Knott and Riggin (41), Hartmann (42) for ICR drift cells and by Sharp et al. (43), McIver et al. (44), Comisarow (45) and Dunbar (46) for ion traps.

An example of the complexity of the frequency variations in the cubic cell is given in the extreme by the splitting of a peak into a doublet for ions excited to very large orbits. A similar phenomenon was noted by Marshall (47). In the example reported here, the ions were excited by a 0.385 volt peak-to-base RF burst in a 0.0254 m cubic cell with a 1 volt trap and a magnetic field of 1.2 T. Two maxima are discernible for ion-cyclotron-orbit sizes larger than the "optimal" orbit size at about 760 µsec excitation time. Local centroids are measurable; one increases by ca. 50 Hz and the other

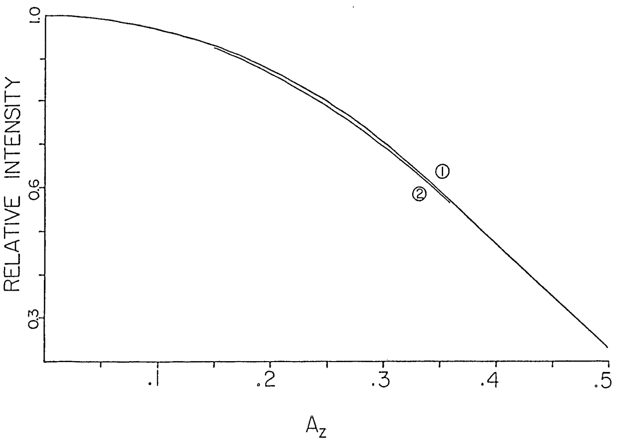

Figure 6. Relative fundamental harmonic amplitude as a function of z-oscillation amplitude. (1) $A_r = 0.25$ when $A_z = 0$. (2) $A_r = 0.05$ when $A_z = 0$. (Reproduced with permission from Ref. 33. Copyright 1986 Elsevier Science Publishers B.V.)

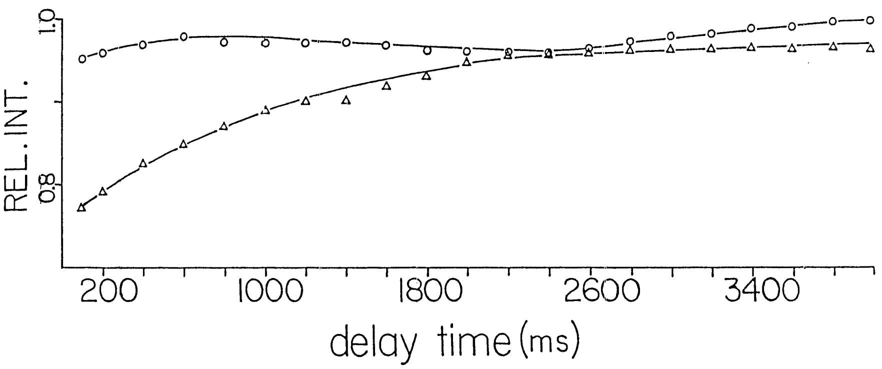

Figure 7. The relative ion signal intensity of an initial 100,000 benzene ions vs. time under conditions of no charge exchange at 1.0 V trap (O) with and (Δ) without employment of ion compression. The initial trap voltage was 0.125 V for (O). (Reproduced with permission from Ref. 33. Copyright 1986 Elsevier Science Publishers B.V.)

---

decreases by mor
frequency as the
If the magne
frequency shift
approximately pro
field component
Dunbar's treatmen
in the z = 0 plan
to increase in
Evaluation of ra
radial positions
frequencies of io
increasing orbit
to ions with low
ions with high z-m

Because low
modify the z-mod
expected to refle
excitation. Thi
hypothesis: by a
ion-molecule coll
change. Indeed, a
the expense of the

The observati
that peaks split
orbit suggest tha
circumstances. C
frequencies for io
there are mass d
populate the trap
mass measurement
cyclotron mode doe
discriminating z-m
chapter. Thus, f
errors are due in p
are evident at lo
excitation induced
number.

Systematic err
because assumption
practice. One of
of Jefferies (49),
that a thermal ion
an oblate ellipsoid
the space charge p
constant contributi
shape of the ion cl
charge electric fie
systematic errors ma
not unexpected. T
excitation compared
the cyclotron orbits
RF burst (50) and ch
the ion distributio
chapter.

decreases by more than 180 Hz away from the "optimal" orbit size frequency as the excitation time is increased.

If the magnetron mode is negligible in size, then the cyclotron frequency shift caused by the radial electric fields is approximately proportional to the magnitude of the radial electric field component divided by the radius, $-E_r/r$ (48). Based on Dunbar's treatment (46), which shows a decrease in the average E_r/r in the z = 0 plane, one would expect ions with low z-mode amplitudes to increase in frequency as their orbit sizes are increased. Evaluation of radial electric trapping fields at larger z and radial positions shows a large increase suggesting that the frequencies of ions with high z-mode amplitudes would decrease with increasing orbit size. Thus, we attribute the high-frequency peak to ions with low z-mode amplitudes and the low-frequency peak to ions with high z-mode amplitudes.

Because low amplitude RF burst waveforms do not significantly modify the z-mode amplitudes of ions, the intensities would be expected to reflect the z-mode amplitude distribution just before excitation. This gives us one means of checking the above hypothesis: by allowing the z-mode amplitudes to relax via ion-molecule collisions, the relative peak intensities should change. Indeed, at long delay, the high frequency peak increases at the expense of the low frequency peak.

The observations that there is an "optimum" orbit size and that peaks split for orbits not too much larger than the optimum orbit suggest that the optimum orbit occurs because of special circumstances. One possible circumstance is a coincidence of frequencies for ions with low and high z-mode amplitudes so that if there are mass discriminating differences in the way the ions populate the trap or in the way ions are excited, then systematic mass measurement errors can be expected. Excitation of the cyclotron mode does produce a spread in cyclotron radii, and mass discriminating z-mode excitation is discussed elsewhere in this chapter. Thus, frequency variations that cause systematic mass errors are due in part to trap field inhomogeneities. These effects are evident at low ion populations and may be due in part to excitation induced ion cloud deformation which increases with ion number.

Systematic errors that increase with ion number occur, perhaps, because assumptions made in the model are being violated in practice. One of the basic assumptions of the space charge theory of Jefferies (49), from which the calibration law was derived, is that a thermal ion cloud in a cubic Penning trap takes the shape of an oblate ellipsoid with a uniform distribution of charge. If so, the space charge potential should be quadratic, thus producing a constant contribution to E_r/r. If excitation were to alter the shape of the ion cloud, and consequently the linearity of the space charge electric field, then the linear model no longer applies, and systematic errors may occur. Altering the shape of the ion cloud is not unexpected. The orbits of ions are known to be large after excitation compared to before excitation, and calculations show that the cyclotron orbits vary by as much as 50% of the largest orbit for RF burst (50) and chirp (25) excitations. z-Excitation also affects the ion distribution in the cell as is discussed earlier in this chapter.

3. Tools: To determine the accuracy of a derived calibration law, computed masses of ions are compared to known values by using the calibration shown in equation (2) for the cubic cell or that shown in equation (3) for the hyperbolic.

$$\text{Hyperbolic cell} \qquad f^2 = a/m^2 + b/m \qquad (3)$$

The values of a and b were determined empirically by measuring the frequencies of six reference masses and fitting mass-frequency data to the form of the equation by means of a least-squares procedure. By using empirical values of a and b and the measured ion frequencies, the masses of the six ions were calculated. A statistical evaluation between the known masses and the experimentally determined masses was then made to determine the accuracy of the calibration law. Systematic errors were observed as is described in (40).

4. Possible Solutions: New cell designs have been investigated as possible solutions for improving accurate mass measurements. Efforts have been directed at minimizing frequency complexity by linearizing the trapping fields and reducing space charge effects by spreading out the ions. The reduction of space charge effects would also permit improvement in dynamic range.

One possibility is the rectangular cell proposed by McIver *et al.* (29). The cell is elongated along the z-axis so that the ion frequencies experience less perturbation associated with the trapping fields. Also because of the large volume in the cell, more ions can be stored with less ion-ion coupling effects than in the cubic cell.

A recent effort of this laboratory has resulted in the introduction of a hyperbolic Penning trap (31). The cell consists of two end caps and one ring electrode similar to the design of Byrne and Farago (51) (see Figure 8).

Ions are formed by an electron beam offset at 1/2 r_o because ions cannot be excited at the center of the cell. This is done also to allow the largest possible cyclotron orbit between the z-axis and the ring electrode. The cyclotron mode of the ions is excited across the ring and end caps, and image currents are detected by using a balanced bridge circuit (52).

The hyperbolic cell offers several advantages for accurate mass determinations. 1) The frequencies of fundamental modes of the ion motion are independent of the location of the ion in the cell at least for the low ion limit. This is important because frequencies are known to be influenced by the location of the ions in cubic cells. 2) The excitation electric field has a simple form identical to that of the trapping field. Thus, the operation of the trap is the same everywhere in the interior permitting most of the volume to be used for storage of larger ion populations with reduced space charge effects. 3) Harmonic effects (31,13b) that complicate spectra are removed.

The mass calibration law gives mass measurement accuracy of ca. 2 ppm and a precision of ca. 1 ppm. Errors are still systematic, but the measurements are much less sensitive to space charge effects than those made with the cubic cell. One possible cause of the systematic errors may be magnetic field inhomogeneity caused by

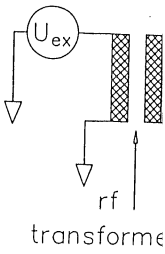

Figure 8. H
network.

ved calibration
values by using
ic cell or that

(3)

ly by measuring
mass-frequency
a least-squares
nd the measured
calculated. A
sses and the
determine the
s were observed

s have been
accurate mass
izing frequency
reducing space
luction of space
mic range.
ed by McIver et
so that the ion
ated with the
ne in the cell,
effects than in

esulted in the
ne cell consists
the design of

1/2 r_o because
his is done also
ween the z-axis
ions is excited
are detected by

or accurate mass
modes of the ion
in the cell at
ause frequencies
e ions in cubic
a simple form
operation of the
ting most of the
ons with reduced
that complicate

accuracy of ca.
till systematic,
e charge effects
le cause of the
neity caused by

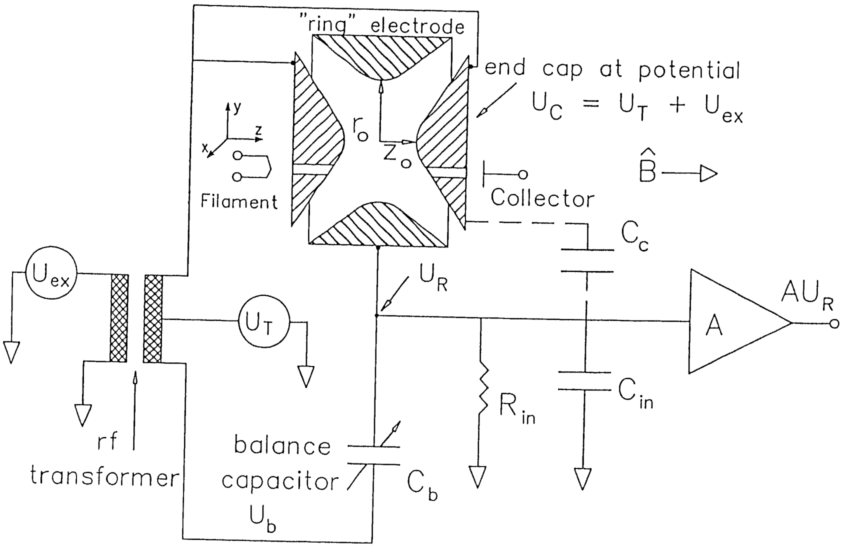

Figure 8. Hyperbolic Penning cell imbedded in a balanced bridge network.

local magnetic fields induced by machining the cell from stainless steel.

Another cell design may incorporate the use of segmented trap plates in the cubic cell (Figure 4) (53). Segmenting the trap plates is expected to minimize trapping field inhomogeneities.

Poor Resolution for High Mass Ions. 1. Problem Definition and Model: The magnitude of the electric forces, both trapping and coulombic, relative to the magnetic force increases with increasing mass. As a result one would expect that any motion problems resulting from electric fields would also increase with ion mass. This may be one of the causes of the low resolution detection of high mass ions (54), particularly organic ions, by FTMS. This problem definition is not intended to detract from the remarkable accomplishments of Hunt, Russell and coworkers which are reported elsewhere in this volume.

The study of high mass ion dynamics is complicated by the relatively poor control over ion populations by methods used to generate high-mass ions (e.g., laser desorption, SIMS) and by the possibility that chemical behavior of the ion (e.g., slow decompositions) will interfere with efforts to gain information about dynamical behavior. We are proposing a scaling technique that may be used to gain experimental insight into the dynamics of high-mass ions. Scaling (55) involves extrapolating information about the dynamics of high-mass ions at high magnetic fields by studying experimentally low mass ions at lower magnetic fields.

2. Model: Consider the phenomenological equation (56) of the motion of the ion to be studied:

$$\frac{d^2\vec{x}}{dt^2} = \frac{q}{m}\ \vec{E}(\vec{x}) + \frac{d\vec{x}}{dt} \times \vec{B} - \zeta\frac{d\vec{x}}{dt} \tag{4}$$

By introducing the coordinate transformations

$$t = (q/m)^{1/2}t \tag{5}$$

$$\vec{\chi}(t) = \vec{x}(t) \tag{6}$$

and parameter changes

$$\vec{\beta} = \vec{B}/(m/q)^{/2} \tag{7}$$

$$\nu = (m/q)^{1/2}\zeta \tag{8}$$

the phenomenological equation becomes

$$\frac{d^2\vec{\chi}}{d\tau^2} = \vec{E}(\vec{\chi}) + \frac{d\vec{\chi}}{d\tau} \times \vec{\beta} - \nu\frac{d\vec{\chi}}{d\tau} \tag{9}$$

Note that the electric field as a function of ion position remains unchanged. The solution, $\vec{\chi}$, of the scaled equation represents the physical solution, $\vec{x}$, for any situations where $\vec{B}/(m/q)^{1/2} = \vec{\beta}$ and $\zeta(m/q)^{1/2} = \nu$. The $\vec{x}$ is recovered from $\vec{\chi}$ by scaling the time variable. Thus, it can be seen that the behavior of two situations for which

must be the s
made. This v
fields can be s
Tool: As
conditions be
scale the equa
into equations
As an exa
consider that a
an ion of m/z
molecular ion a
the behavior of
to the behavior
The scalin
results at this
problem.

Low Mass Re
Experiments. 1.
MS/MS and parti
of problem-solv
resolution for c
been demonstrate
However, the res
cells is poor.
limited to the
involving high m
is ejected, ex
disadvantage pe
instruments, but
possible to reta
both the MS-I an
ions in the fir
information on o
particularly whe
production is poo
2. Model:
daughter ions in
which one can sel
difference betwee
MS step, the sig
after the concl
particular peak
inhomogeneities o
excitation is co
change the ampli
during this time
contained in a p
first MS step,
accelerating one
a neighbor mass s
the excitation.
bounded close to

$$\vec{B}/(m_2/q)^{1/2} = \vec{B}/(m_2/q)^{1/2} \qquad (10)$$

must be the same after the appropriate time scale adjustment is made. This would suggest high mass behavior at high magnetic fields can be studied with low mass ions at low magnetic fields.

Tool: As a tool, scaling requires that experimental conditions be chosen that imitate the variable changes required to scale the equations for a high mass ion at a high magnetic field into equations for a low mass ion at a lower magnetic field.

As an example of how mass scaling would be used as a tool, consider that an investigation directed nominally at the dynamics of an ion of m/z 2000 at 3 T can be made by using the benzene molecular ion at 0.59 T. By analogy, it should be possible to study the behavior of low mass ions and relate that information directly to the behavior of high mass ions at high magnetic fields.

The scaling approach is at the proposal stage, and we have no results at this time and no detailed solutions to suggest for the problem.

Low Mass Resolution Ion Selection for MS-I in MS/MS Experiments. 1. Problem Definition: The advantages of FTMS for MS/MS and particularly for $(MS)^n$ are often touted, yet few reports of problem-solving in chemical analysis have been made. The mass resolution for daughter ions can be superb in the MS/MS mode, as has been demonstrated by Wilkins et al. (57) and Freiser et al. (58). However, the resolution of MS-I (for parent ion selection) in cubic cells is poor. Moreover, the energy for collisional activation is limited to the cyclotron mode energy and this limits applications involving high mass ions. Finally, the original population of ions is ejected, except for the ion of interest. This latter disadvantage pertains also to sector and quadrupole tandem instruments, but it need not apply to FTMS. That is, it should be possible to retain some of the "multichannel advantage" of FTMS in both the MS-I and the MS-II modes by not throwing away most of the ions in the first MS step. It may be highly desirable to obtain information on other ionic species from the original ion population particularly when sample sizes are limited in quantity or when ion production is poor and a limiting factor.

2. Model: The difference between the mass resolution of daughter ions in the second MS step and the mass resolution with which one can select the parent ion in the first MS step is due to a difference between the operations of these two steps. In the second MS step, the signals that result in the mass spectrum are observed after the conclusion of the excitation. So the width of a particular peak in the spectrum is determined by trap field inhomogeneities of the regions through which the ions pass after the excitation is complete. Because only collisional processes will change the amplitudes of the z, magnetron, and cyclotron modes during this time, one would expect the ion trajectories to be contained in a proper subset of the volume of the cell. In the first MS step, the ejection resolution describes the limits for accelerating one ion species to the point of ejection while leaving a neighbor mass species essentially undisturbed at the conclusion of the excitation. The act of accelerating an ion that is initially bounded close to the z-axis to an ion with a large cyclotron mode

for ejection requires the ion to move through a large portion of the trap volume. As a result, the motion of the ion is affected by the full extent of the trap field inhomogeneities. By this reasoning, the resolutions of the two MS steps would be different, and the ejection resolution of the first MS step would be poorer.

For low ion populations, a first estimate of achievable ejection resolution might be obtained from the cyclotron frequency spread that occurs over the range of cyclotron orbit radii through which the ion must pass to be ejected. This is based on the notion that an ejection waveform that is just adequate to eject one ion must have a frequency spectral peak that is at least as wide as the above spread of frequencies. Such a waveform would then excite, at least to some extent, all ions with frequencies falling within the width of the peak, thus limiting the ejection resolution. For ions with low z-mode amplitudes, we can use Dunbar's (46) approximate expression for the average radial field strength,

$$E_r \simeq 2\alpha(V_T/a^2)\, r\, [1-2.8(r^3/a^3)] \qquad (11)$$

to obtain the frequency spread between the smallest and largest orbit:

$$\Delta\omega_{eff} \simeq 0.7(qB/m_c)(r_m/a)^3 \qquad (12)$$

Here, B is the magnetic field strength, m_c is the critical mass (40), q is the charge of the ion in question, r_m is the maximum radius required for ejection, a is the inside length of the cubic cell, r is a radial displacement, V_T is the voltage applied to the trap plates, and $\alpha = 1.3871$ (49) a geometry constant.

In the derivation of the approximate expression for $\Delta\omega_{eff}$, use was made of

$$\Delta_{eff} = 1/2\ qB/m\ \{1 + [1-4(m/q)(E_r/r)/B^2]1/2\} \qquad (13)$$

for the cyclotron frequency of an ion of mass, m, with an orbit centered on the z-axis, and

$$m_c/q = q^2B^2/8\alpha\nu_T \qquad (14)$$

for the critical mass (upper bound on the range of ion masses for which the ion trajectory is stable in the trap).

From the expression for $\Delta\omega_{eff}$, the ejection resolution becomes

$$m/\Delta m \simeq \omega_{eff}/\Delta\omega_{eff} \simeq 1.429(m_c/m)(a/r_m)^3 \qquad (15)$$

As an example, in a 2.54 cm cubic trap with B = 1.2 T and V_T = 1 V, the above estimate for the ejection resolution gives 1.59 K.

3. Tool: RF burst waveforms serve as a convenient means for determining the ejection resolution limits that are due to effects intrinsic in the operation of the cubic trap. More general computed waveforms (59) are obtained via inverse discrete Fourier transformation. These computed waveforms are just a linear superposition of a finite number of RF bursts. As a result, it is proposed that the best performance obtained with RF bursts anticipate the best performance obtained with computed waveforms,

---

when these wavef
burst is the spe
that is best suit
The MS-1 res
spectra. These s
bursts, the firs
quantitates the n
ion signal intens
the frequency is
ion resonance, th
the ejection resol
The first st
resolution limits
waveform time - a
complete loss of i
of the test wavef
peak width in the
enough to cover t
ion.
Then, in ste
maintaining the c
minimum of the eje
shows a complete l
width of the dip i
were functioning as
no collisional damp
increased without e
dip minimum.
By using this
the example given i
2.4 K. This compar
the same trap condit
4. Proposed
possibility of an
storing all ions fr
may be accomplished
manner similar to t
trap plate would no
(see Figure 9). The
diameter of 1/2 the
by a highly transpa
from the disk so th
than that of the dis
Electrons (or
left through an ori
They would strike t
tandem. Ionization
begin the experimen
traps by using the p
(60) or even more ef
similar to those desc
Once the ion po
population is again l
a cyclotron orbit sli
the supporting scree

when these waveforms are used for ejection. In particular, the rf burst is the special case in the class of all computed waveforms that is best suited for ejection of a single mass.

The MS-1 resolution is determined through the use of ejection spectra. These spectra are produced in an experiment using two rf bursts, the first is the test ejection waveform and the second quantitates the number of unejected ions. The spectra are plots of ion signal intensity versus the frequency of the test waveform as the frequency is stepped through the resonance of the ion. At the ion resonance, the plot shows a dip having a width that indicates the ejection resolution of the test waveform.

The first step in the measurement of the intrinsic ejection resolution limits of the trap is to find the minimum ejection waveform time - amplitude product for which the dip minimum shows complete loss of ion signal. This is done by varying the amplitude of the test waveform and fixing the time at ~1 msec to assure the peak width in the frequency spectrum of the test waveform is wide enough to cover the range of cyclotron frequencies of the ejected ion.

Then, in steps, the test waveform time is increased while maintaining the original time-amplitude product until the dip minimum of the ejection spectrum acquired for each step no longer shows a complete loss of ion signal. At this step, the half-height width of the dip is used to determine the resolution. If the trap were functioning as an ideal trap, that is, as a linear device with no collisional damping, the test waveform time could be indefinitely increased without ever showing incomplete loss of ion signal at the dip minimum.

By using this technique, the ejection resolution measured for the example given in the "Model" section is certainly no better than 2.4 K. This compares with a normal mass resolution of 30 K under the same trap conditions.

4. Proposed Solution: We suggested earlier (9) the possibility of an intermediate cell in MS/MS applications for storing all ions from which the one of interest is selected. This may be accomplished by assembling two adjoining cubic cells in a manner similar to that in (60) except the partitioning or center trap plate would not contain an orifice but rather be a solid disk (see Figure 9). The disk would be centered on the z-axis and have a diameter of 1/2 the cell dimension. The disk will be held in place by a highly transparent metallic screen or grid that is insulated from the disk so that it can be operated at a potential different than that of the disk.

Electrons (or any ionizing beam) would be admitted from the left through an orifice in the trapping plate opposite the disk. They would strike the disk after traversing the first cell of the tandem. Ionization of a pulsed sample (from a pulsed valve) would begin the experiment although ions may be introduced from other traps by using the partitioning principle of the Nicolet dual cell (60) or even more effectively by employing ion transfer techniques similar to those described over twenty years ago (51).

Once the ion population is formed and stable and the neutral population is again low, the ions to be activated are accelerated to a cyclotron orbit slightly larger than the disk. Up to this point, the supporting screen and disk have been at the same trapping

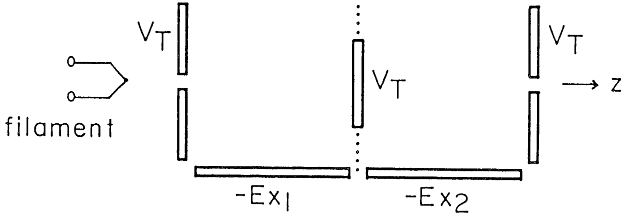

Figure 9. Proposed segmented cell with disk shaped center trap plate.

---

potential, bu
described in
cell. The
sufficiently
disk.

The sel
nominally to
though this
sufficiently
performed.

Ion acti
ions, electro
These activat
their traject
first cell are

The segme
1) The origin
currently the
z-axis, and t
process. 3)
resolution bec
a/r_m in Equat
generated by
plate potentia
excitation).
cyclotron mode
shielded from

Conclusions

Most FTMS ins
focussed on de
FTMS with var
supercritical
pulsed SIMS, C
various inter
demonstrations
potential of th
of FTMS for tr
determination o
mass spectromet
Another is that
experiments hav
highly focussed

We propose
of FTMS is t
spectrometric
determination o
this paper, fiv
height measurem
inadvertant z-ej
because of ion
measurement erro
positions. Less
for ejecting i

potential, but now the screen is pulsed in a fashion similar to that described in (60,61) to transfer the excited ion to an adjoining cell. The z-mode motion of the unexcited ions is not disturbed sufficiently to climb the potential barrier still provided by the disk.

The selected ions now in the adjoining cell are returned nominally to the z-axis by using the method of Marshall (62). Even though this deexcitation may not be perfect, it should be sufficiently adequate that the next step of ion activation can be performed.

Ion activation takes place by admitting particles (photons, ions, electrons) into the cell containing the ion of interest. These activating particles are injected along the z-axis so that their trajectory is interrupted by the disk, and the ions in the first cell are preserved.

The segmented tandem cell should have the following advantages: 1) The original population of ions is not lost by ejection as is currently the case. 2) The selected ions are activated along the z-axis, and this should lead to better performance in the MS-II process. 3) The ion of interest can be selected at higher mass resolution because the selection radius is kept small (increased a/r_m in Equation 15) and because better trapping fields can be generated by the disk/screen arrangement (the outer segment trap plate potential would be set for minimum ion frequency spread during excitation). 4) The activation energy is not limited to the cyclotron mode energy. 5) The original population of ions is shielded from the activation process.

ter trap

Conclusions

Most FTMS instrument and method development research has been focussed on demonstration experiments. Examples include coupling FTMS with various sample introduction schemes (e.g., GC, LC, supercritical fluid chromatography), sample ionization (e.g., LD, pulsed SIMS, Cf-252 PDMS, etc.), and demonstrating application to various interesting classes of chemical compounds. These demonstrations are useful because they are indications of the potential of the technique. However, few reports of the routine use of FTMS for trace analysis, for accurate mass, and for structure determination of unknowns have yet appeared. One reason is that FT mass spectrometers are not widely spread in the hands of users. Another is that FTMS is not yet routine. Most of the demonstration experiments have been done in expert laboratories by committed and highly focussed graduate students and postdoctoral researchers.

We propose that an essential route to the routine utilization of FTMS is to focus on fundamental issues that face any spectrometric method; that is, issues dealing with accurate determination of peak position, peak shape, and peak height. In this paper, five problems were introduced. With regard to peak height measurements are problems of nonuniform tuning owing to inadvertant z-ejection of ions and temporal variation of ion signals because of ion cloud relaxation phenomena. Systematic mass measurement errors are an example of problems in determining peak positions. Less than optimum resolutions for high mass ions and for ejecting ions in MS/MS-type experiments are examples of peak-shape difficulties. In all cases, approaches to solving the problems are given and, in many cases, actual solutions are presented.

Acknowledgments

This work was supported in part by the Midwest Center for Mass Spectrometry (NSF Grant CHE-8620177).

Literature Cited

1. Svec, H.J. Int. J. Mass Spectrom. Ion. Proc., 1985, 66, 3.
2. Thomson, J.J., Rays of Positive Electricity and the Application to Chemical Analyses; Longmans Green: London, 1913.
3. Dempster, A.J., Phys Rev, 1918, 11, 316.
4. Aston, F.W., Philos. Mag. VI, 1919, 18, 707.
5. Bartky, W.; Dempster, A.J., Phys. Rev., 1929, 33, 1019.
6. Cottrell, J.S.; Greathead, R.J., Mass Spectrom. Rev., 1986, 5, 215.
7. a. Bateman, R.H.; Burns, P.; Owen, R.; Parr, V.C., Adv. Mass Spectrom., 1986, 1013, 863. b. Bateman, R.H.; Owen, R.; Parr, V.C.; Wood, D., Proceedings of the 34th Annual Conference on Mass Spectrometry and Allied Topics, 232, 1986.
8. Comisarow, M.B.; Marshall, A.G., Chem. Phys. Lett., 1974, 25, 282.
9. a. Comisarow, M.B.; Marshall, A.G., J. Chem. Phys., 1976, 64, 110. b. Gross, M.L.; Rempel, D.L., Science, 1984, 226, 261.
10. Ogata, K.; Matsuda, H., Z. Naturforsch. Teil A, 1955, 10, 843.
11. Allemann, M.; Kellerhals, Hp.; Wanczek, K.-P., Int. J. Mass Spectrom. Ion Phys., 1983, 46, 139.
12. Laude, D.A.,Jr.; Johlman, C.L.; Brown, R.S.; Weil, D.A.; Wilkins, C.L., Mass Spectrom. Revs., 1986, 5, 107.
13. a. Comisarow, M.B., J. Chem. Phys., 1978, 69, 4097. b. Nikolaev, E.N.; Gorshkov, M.V., Int. J. Mass Spectrom. Ion Proc., 1985, 64, 115.
14. a. Amster, I.J.; McLafferty, F.W.; Castro, M.E.; Russell, D.H.; Cody, R.B., Jr.; Ghaderi, S., Anal. Chem., 1986, 58, 483. b. Russell, D.H., Mass Spectrom. Rev., 1986, 5, 167.
15. Aberth, W., Anal. Chem., 1986, 58, 1221.
16. McCrery, D.A.; Sack, T.M.; Gross, M.L., Spectroscopy: An International Journal, 1984, 3, 57.
17. Ghaderi, S.; Kulkarni, P.S.; Ledford, E.B., Jr.; Wilkins, C.L.; Gross, M.L., Anal. Chem., 1981, 53, 428.
18. Laude, D.A., Jr.; Johlman, C.L.; Brown, R.S.; IJames, C.F.; Wilkins, C.L., Anal. Chim. Acta, 1985, 178, 67.
19. Sack, T.M.; Gross, M.L., Anal. Chem., 1983, 55, 2419.
20. Sack, T.M.; McCrery, D.A.; Gross, M.L., Anal. Chem., 1985, 57, 1290.
21. McCrery, D.A.; Peake, D.A.; Gross, M.L., Anal. Chem., 1985, 57, 1181.
22. Peake, D.A., Ph.D. Thesis, University of Nebraska - Lincoln, 1986.
23. Huang, S.K.; Rempel, D.L.; Gross, M.L., Int. J. Mass Spectrom. Ion Proc., 1986, 72, 15.

---

24. Sack, T
1985.
25. Huang, S
26. Beaucham
123.
27. Sherman,
the 31st
Topics,
28. Wang, T.
Proc., 1
29. Hunter,
Spectrom
30. Lee, S.
Spectrom
31. Rempel,
Anal. Che
32. Clow, R.
1972, 8,
33. Rempel, I
Ion Proc.
34. (a) Riggi
Bloom, M.
35. (a) Dehme
109. (b
40, 3421.
6. (d)
G.H., Phy
36. Dunbar, R
37. Ledford,
Kulkarni,
52, 463.
38. Allemann,
Lett., 19
39. Francl, T
W.D.; McI
1983, 54,
40. Ledford,
1984, 56,
41. Knott, T.
42. Hartmann,
Chem. Phys
43. Sharp, T.
Phys., 197
44. a. Shermar
of the 31
Topics, 1
R.L.; Loc
Mass Spect
45. Comisarow,
Spectromet
Verlag, Be
46. Dunbar, R.
Ion Proc.,
47. Marshall,

to solving the
solutions are

enter for Mass

85, 66, 3.
city and the
reen: London,

, 1019.
Rev., 1986, 5,

/.C., Adv. Mass
Owen, R.; Parr,
l Conference on

ett., 1974, 25,

hys., 1976, 64,
34, 226, 261.
1955, 10, 843.
, Int. J. Mass

.; Weil, D.A.;
07.
8, 69, 4097.
s Spectrom. Ion

I.E.; Russell,
hem., 1986, 58,
36, 5, 167.

Spectroscopy: An

Jr.; Wilkins,

IJames, C.F.;

2419.
Chem., 1985, 57,

Chem., 1985, 57,

aska - Lincoln,

. Mass Spectrom.

24. Sack, T.M., Ph.D. Thesis, University of Nebraska-Lincoln, 1985.
25. Huang, S.K.; Rempel, D.L.; Gross, M.L., unpublished work.
26. Beauchamp, J.L.; Armstrong, J.T., Rev. Sci. Instrum., 1969, 40, 123.
27. Sherman, M.G.; Francl, T.J.; McIver, R.T., Jr., Proceedings of the 31st Annual Conference on Mass Spectrometry and Allied Topics, 1983, 400.
28. Wang, T.C.L.; Marshall, A.G., Int. J. Mass Spectrom. Ion Proc., 1986, 68, 287.
29. Hunter, R.L.; Sherman, M.G.; McIver, R.T., Int. J. Mass Spectrom. Ion Phys., 1983, 50, 259.
30. Lee, S.H.; Wanczek, K.-P.; Hartman, H., Advances in Mass Spectrometry, 1980, 8B, 1645.
31. Rempel, D.L.; Ledford, E.B.,Jr.; Huang, S.K.; Gross, M.L., Anal. Chem, In press.
32. Clow, R.P.; Futtrell, J.H., Int. J. Mass Spectrom. Ion Phys., 1972, 8, 119.
33. Rempel, D.L.; Huang, S.K.; Gross, M.L., Int. J. Mass Spectrom. Ion Proc., 1986, 70, 163.
34. (a) Riggin, M.; Woods, I.B., Can J. Phys., 1974, 52, 456. (b) Bloom, M.; Riggin M., Can. J. Phys., 1974, 52, 436.
35. (a) Dehmelt, H.G., Adv. At. Mol. Phys., 1967, 40, 53; 1969, 5, 109. (b) Church, D.A.; Dehmelt, H.G., J. Appl. Phys., 1969, 40, 3421. (c) Church, D.A.; Mokri, B., Z. Phys., 1971, 224, 6. (d) Heppner, R.A.; Walls, F.L.; Armstrong, W.T.; Dunn, G.H., Phys. Rev. A, 1976, 13, 1000.
36. Dunbar, R.C., Int. J. Mass Spectrom. Ion Proc., 1984, 56, 1.
37. Ledford, E.B.,Jr.; Ghaderi, S.; White, R.L.; Spencer, R.B.; Kulkarni, P.S.; Wilkins, C.L.; Gross, M.L., Anal. Chem., 1980, 52, 463.
38. Allemann, M.; Kellerhals, Hp.; Wanczek, K.-P., Chem. Phys. Lett., 1981, 84, 547.
39. Francl, T.; Sherman, M.G.; Hunter, R.L.; Locke, M.J.; Bowers, W.D.; McIver, R.T., Jr., Int. J. Mass Spectrom. Ion Proc., 1983, 54, 189.
40. Ledford, E.B.,Jr.; Rempel, D.L.; Gross, M.L., Anal. Chem, 1984, 56, 2744.
41. Knott, T.F.; Riggin, M., Can. J. Phys., 1974, 52, 426.
42. Hartmann, H.; Chung, K.-M.; Baykut, G.; Wanczek, K.-P., J. Chem. Phys., 1983, 78, 424.
43. Sharp, T.E.; Eyler, J.R.; Lie, E., Int. J. Mass Spectrom. Ion Phys., 1972, 9, 421.
44. a. Sherman, M.G.; Francl, T.J.; McIver, R.T., Jr., Proceedings of the 31st Annual Conference on Mass spectrometry and Allied Topics, 1983, 400. b. Francl, T.J.; Sherman, M.G.; Hunter, R.L.; Locke, M.J.; Bowers, W.D.; McIver, R.T., Jr., Int. J. Mass Spectrom. and Ion Proc., 1983, 54, 189-199.
45. Comisarow, M.B., in Lecture Notes in Chemistry, 31, ICR Spectrometry II, H. Hartmann and K.-P. Wanczek, eds., Springer Verlag, Berlin, 1982, 484.
46. Dunbar, R.D.; Chen, J.H.; Hays, J.D., Int. J. Mass Spectrom. Ion Proc., 1984, 57, 39.
47. Marshall, A.G., J. Chem. Phys., 1971, 55, 1343.

48. Davidson, R.C., Theory of Non Neutral Plasmas, W.A. Benjamin, Reading, Massachusetts, 1974.

49. Jeffries, J.B.; Barlow, S.E.; Dunn, G.H., Int. J. Mass Spectrom. Ion Proc., 1983, 54, 169.

50. Rempel, D.L.; Huang, S.K.; Gross, M.L., Int. J. Mass Spectrom. Ion Proc., 1986, 70, 163.

51. Byrne, J.; Farago, P.S., Proc. Phys. Soc., 1965, 86, 801.

52. McIver, R.T., Jr.; Hunter, R.L.; Ledford, E.B., Jr.; Locke, M.J.; Francl, T.J., Int. J. Mass Spectrom. Ion Phys., 1981, 39, 65.

53. Huang, S.K.; Rempel, D.L., Proceedings of the 34th Annual Conference on Mass Spectrometry and Allied Topics, 1986, 167.

54. a. Amster, I.J.; McLafferty, F.W.; Castro, M.E.; Russell, D.H.; Cody, R.B., Jr.;Ghaderi, S., Anal. Chem., 1986, 58, 483.
b. Hunt, D.F., private communication.

55. Arnold, V.I., Geometric Methods in the Theory of Ordinary Differential Equations, Springer Verlag, 1983.

56. Beauchamp, J.L., J. Chem. Phys., 1966, 46, 1231.

57. White, R.L.; Wilkins, C.L., Anal. Chem., 1982, 54, 2211.

58. Cody, R.B.; Freiser, B.S., Anal. Chem., 1982, 54, 1431.

59. Marshall, A.G.; Wang, T.C.L.; Ricca, T.L., J. Am. Chem. Soc., 1985, 107, 7893.

60. Cody, R.B.; Kinsinger, J.A.; Ghaderi, S.; Amster, J.J.; McLafferty, F.W.; Brown, C.E., Anal. Chim. Acta., 1985, 178, 43.

61. Schwinberg, P.B.; Van Dyck, R.S., Jr.; Dehmelt, H.G., Phys. Rev. Lett., 1981, 47, 1679.

62. Marshall, A.G.; Wang. T.-C.; Ricca, T.L., Chem. Phys. Lett., 1984, 105, 234.

RECEIVED June 15, 1987